Reprinted from Preprint Volume: 13th Conference on Severe Local Storms, October 17-20, 1983, Tulsa, Okla. Published by the American Meteorological Society, Boston, Mass.

P2.11

ANALYSIS OF WET MICROBURSTS BY DUAL-DOPPLER AND GROUND PHOTOGRAPHY

Brian E. Smith and Brian R. Waranauskas
The University of Chicago
Chicago, Illinois

1. INTRODUCTION

Downbursts, discovered by Fujita in 1976, have posed a problem for aviation because of the large horizontal wind shear and vertical downflow that could be encountered by aircraft (Fujita and Byers, 1977; Fujita and Caracena, 1977; NTSB, 1983), as well as a problem for the general public because of the destructive winds that can occur (Fujita and Wakimoto, 1981).

Two research projects have been implemented to study downburst phenomena: NIMROD in 1978 and JAWS in 1982. As shown by Fujita and Wakimoto (1983a), downbursts can be subdivided into two scales: macrobursts and microbursts. By definition, a macroburst is a large downburst with an outflow diameter of 4 km or greater, while a microburst is a small scale downburst with outflow size less than 4 km. Fujita and Wakimoto (1983a) have shown the existence of both wet and dry microbursts/macrobursts. A wet downburst of either scale is defined to be one which is accompanied by 0.01 or greater inches of rain measured at the surface between the onset and the end of the high winds.

This paper presents examples of wet macrobursts and microbursts from the JAWS Project as seen from dual-Doppler analysis and ground photography, and examines the implications of these outflows in meteorological and aeronautical contexts.

2. VISUALLY IMPRESSIVE WEAK MICROBURSTS

2.1 July 9 Shower near Stapleton Airport

Visual observations during the JAWS Project showed that dangerous-looking showers at the surface may produce weak velocity outflows. One such example was the microburst that occurred on 9 July 1982. A rain shower developed west of Stapleton Airport around 1430 MDT and moved east-northeastward into the JAWS network area. Doppler radars scanned the storm, and a ground chase team team photographed the shower as it moved near Stapleton Airport. A well-defined rainshaft was evident in the rear of the storm (Fig. 1). PAM station data revealed the existence of a microburst with a peak windspeed of 14.2 m/s, during the heavy rain (Fig. 2).

Radar analysis for the time of the microburst is given in Fig. 3. The storm had reflectivities greater than 70 dBZ, indicating that some of the precipitation was hail. Dual-Doppler analysis of the ground-relative flow shows a

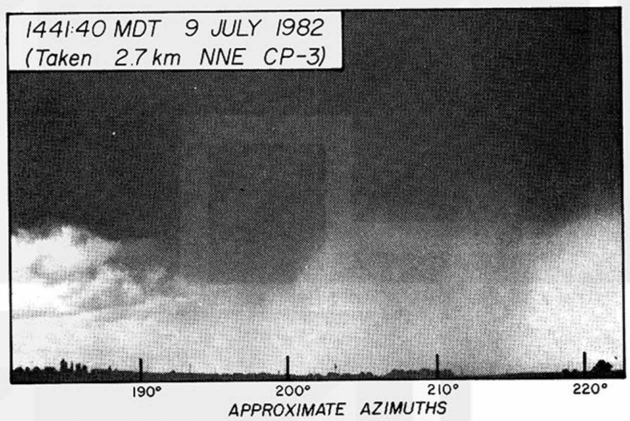

Fig. 1. Rain shaft on 9 July viewed NNE of CP-3 radar site. Photo by T.T. Fujita.

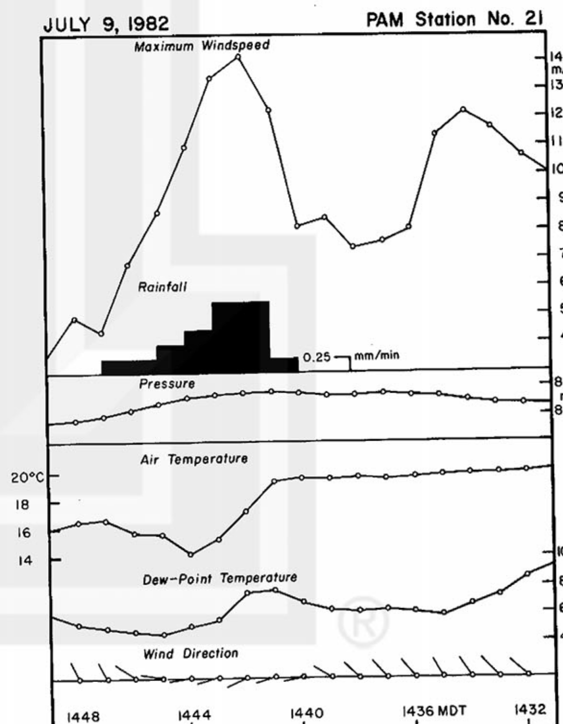

Fig. 2. PAM station time section of 9 July microburst. Maximum speed was 14.2 m/s at 1442 MDT and correlates well with the heaviest rainfall.

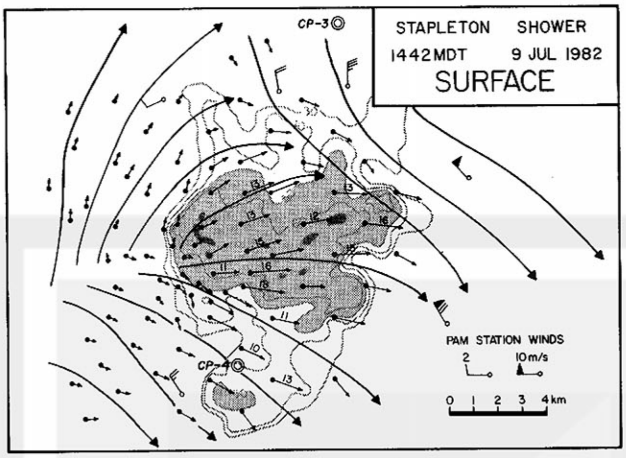

Fig. 3. Ground-relative dual-Doppler velocities of 9 July shower. Gray areas indicate radar reflectivities. Doppler derived velocities are in m/s.

large scale outflow diverging around the backside of the storm. This velocity pattern may be the result of an obstruction flow around the reflectivity core . Imbedded within the core are the strongest velocities of 16-18 m/s. The highest velocities are pointing towards the direction of storm propagation. Storm-relative analysis may reveal a more omnidirectional diverging outflow pattern.

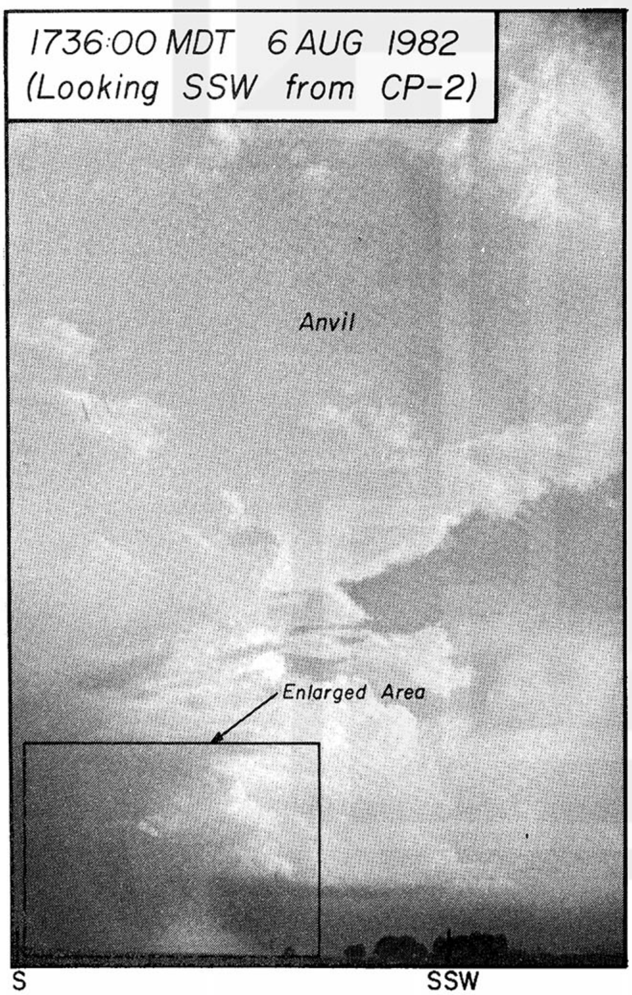

Fig. 4. Thunderstorm viewed SSW of the CP-2 site on 6 August. Photo by T.T. Fujita.

2.2 Rainstorm on August 6

A better example of a strong storm with weak outflow took place west of the JAWS network on 6 August. Fig. 4 shows a photograph of the thunderstorm with an impressive looking precipitation shaft on the front (west) side of the storm. Fig.5 shows an enlargement of the precipitation shaft area. This storm produced rainfall amounts up to 59.4 mm (2.34 inches) west of downtown Denver.

From the photograph in Fig. 5 it would seem that the outflow associated with the storm is quite strong. However, surface dual-Doppler velocities indicate an overall outflow of only 10 m/s. As in the previous example, strong reflectivities and dangerous-looking showers are not necessarily indicative of high velocity outflows at the surface

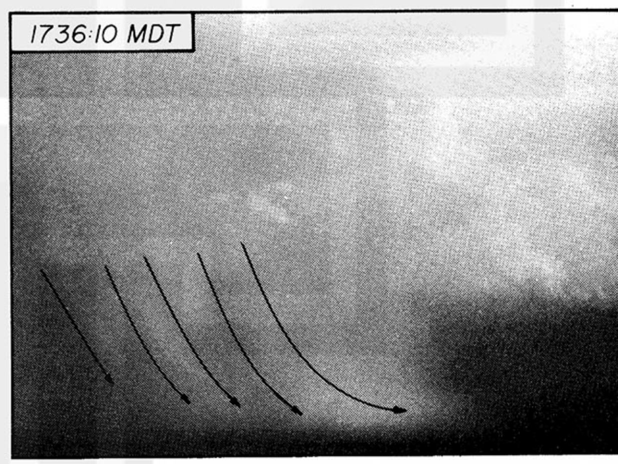

Fig. 5. Enlargement of rain shaft of Fig. 4. Arrows indicate the flow of the falling precipitation. Photo by T.T. Fujita.

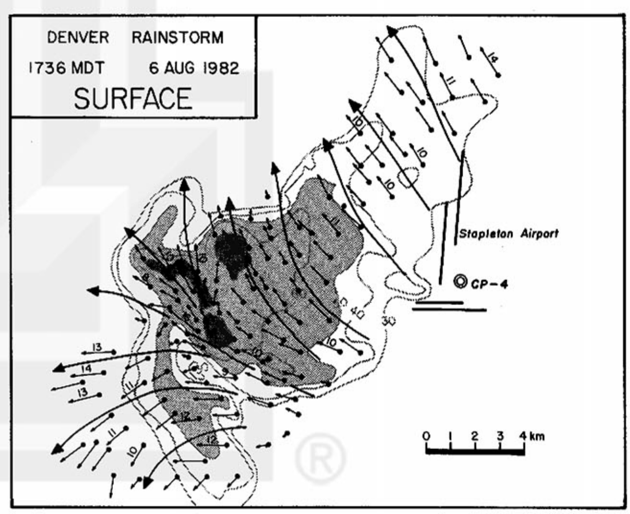

Fig. 6. Ground-relative dual-Doppler analysis of the storm in Figs. 4 and 5. Gray areas indicate reflectivities. Note the high reflectivity area has weak outflow. Doppler derived velocities are in m/s.

3. WET MICROBURSTS WITH STRONG OUTFLOWS

3.1 Microburst of 14 June

On 14 June, large microburst-producing storms formed in the early afternoon throughout the JAWS network. At 1306 MDT a strong cell produced a wet microburst at the north end of runway 35 at Stapleton Airport. As shown in Fig. 7, the maximum outflow speed reached 19 m/s at the surface. Although no rainfall occurred at or before 1306 MDT, the precipitation which began at 1307 MDT was as high as 1.25 mm/min four minutes after microburst detection on the ground.

Observe in Fig. 7 the location of the microburst in relation to the storm reflectivity core. Most of the outflow is ahead of the 60 dBZ reflectivity region. As demonstrated by the dual-Doppler wind field at the surface, the front-side microburst winds are oriented in a NNW-SSE direction, while to the north of the 60 dBZ core the winds are northwesterly and shifting to the west, producing a horizontal shear zone. Single-Doppler velocity patterns at upper levels indicated miso- and mesoscale shearing north of the center of the main cell; this may be significant in microburst production.

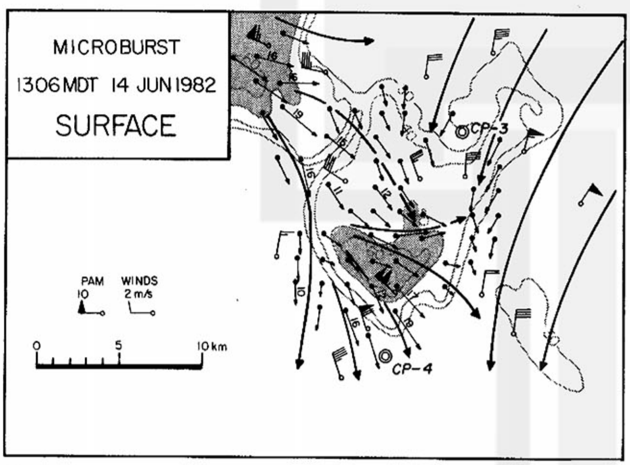

Fig. 7. Surface dual-Doppler wind field of the 14 June microburst. Gray areas are storm reflectivities, and Doppler wind vectors are in m/s.

3.2 Wet Macroburst of 30 June

One of the most impressive wet outflow cases during the JAWS Project occurred on 30 June. A strong microburst descended to the ground at 1820 MDT approximately 8 km northeast of Stapleton Airport and rapidly grew to macroburst size. PAM station no. 23, 4 km to the east of the touchdown point, recorded a peak wind of 29 m/s at 1831 MDT (Fig. 8). Another important feature presented in the PAM data for this station was the rainfall rate (not shown). Unlike the 14 June case (not shown), precipitation occurred before and during the peak wind period. However, similar to the 14 June case, the maximum rainfall rate took place after the time of the peak windspeed. For the outflow period on 30 June, the maximum rainfall rate (0.75 mm/min) and the total rainfall (2.50 mm) were less than these values for 14 June (1.25 mm/min and 4.75 mm, respectively). This supports the finding that there appears to be no correlation between the rainfall rates and outflow windspeeds (Fujita and Wakimoto, 1983a).

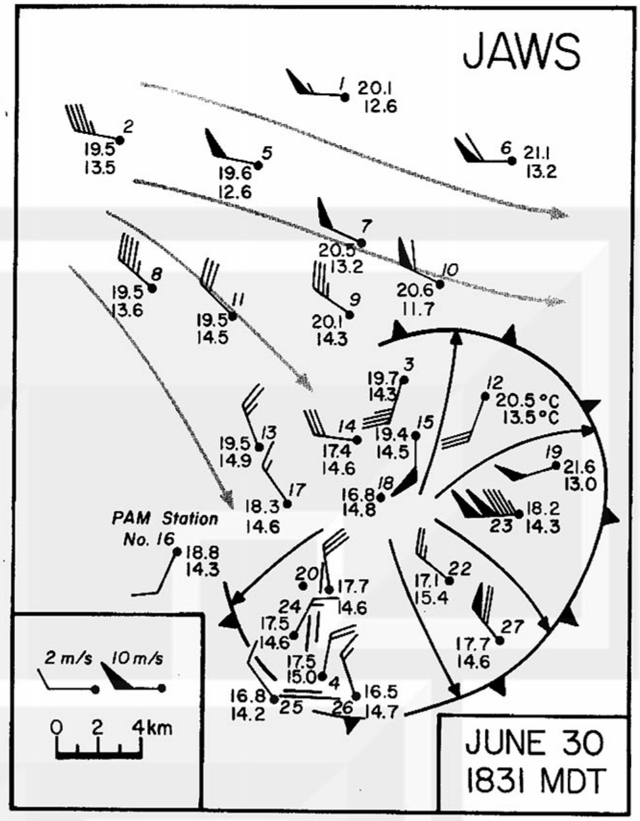

Fig. 8. PAM station winds for the 30 June macroburst at 1831 MDT. Note that the diameter of the downburst is already greater than 15 km only 11 minutes after touchdown.

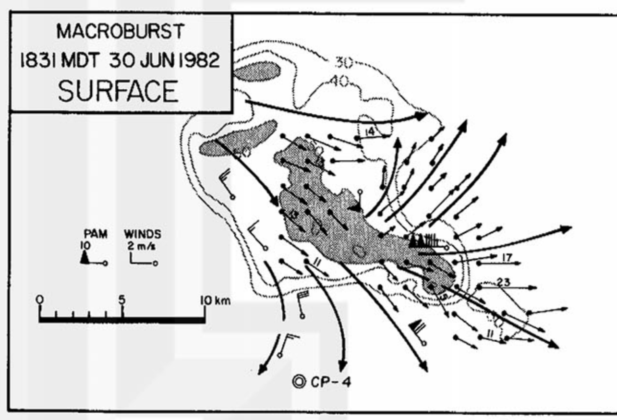

Fig. 9. Dual-Doppler wind field at the surface for the 30 June macroburst at 1831 MDT. Reflectivities are represented by the gray isolines, and the Doppler vectors are in m/s.

Reflectivity and dual-Doppler velocity patterns of the macroburst stage of the outflow from the 30 June storm are presented in Fig. 9. Inspection of Fig. 9 details similar characteristics between this case and the storm on 14 June. As in the 14 June storm, the diverging outflow area on 30 June is away from the 50 dBZ core. Also, the winds north of the 50 dBZ region show marked cyclonic vorticity, an indication that in both cases the outflows may be spiraling outward from the high reflectivity area. Preliminary upper-level dual-

Doppler analysis shows a possible misocyclone just north of the macroburst position at the surface, suggesting that rotation aloft may play a role in wet microburst formation just as they do in some dry cases (Fujita and Wakimoto, 1983a).

4. MICROBURST WIND SHEAR

Aircraft that penetrate a microburst during landing and takeoff may encounter serious flight performance problems. Fujita and Wakimoto (1983b) devised a model for calculating the maximum wind shear that an aircraft would encounter flying through the center of a microburst. A diagram of the type of wind shear affecting an airplane entering a microburst is shown in Fig. 10. The largest vector difference between the headwind and tailwind components along a flight path through the center of a microburst gives the maximum shear experienced by an aircraft.

A plot of the maximum wind shear for various angles relative to the front side of the microburst is shown in Fig. 11, derived from the 9 July case. The greatest shear occurs in the same direction as that of the storm propagation, while the weakest shear takes place in a direction normal to the storm movement.

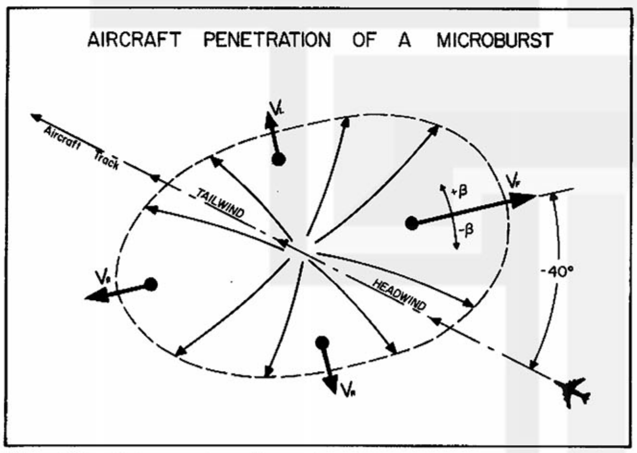

Fig. 10. Schematic of a microburst viewed in the horizontal plane with an aircraft entering at angle β = -40° (angle right or left of maximum front-side wind, V_F). V_F, V_B, V_L, and V_R are the front, back, left, and right maximum winds respectively.

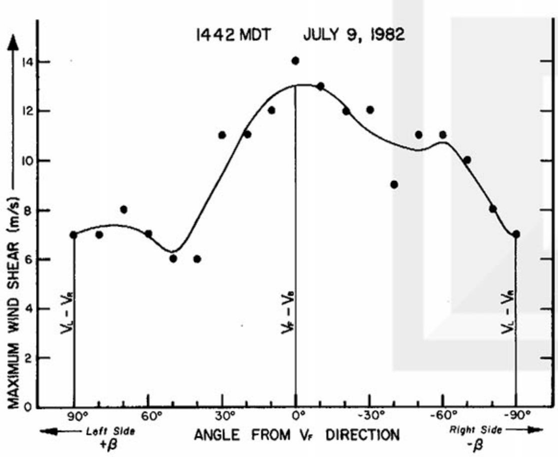

Fig. 11. Maximum wind shear calculated for the 9 July shower for various angles of β. Note that the strongest shear is at 0°, in the direction of storm movement.

5. CONCLUSIONS

Analysis of ground photographs and radar data of wet microbursts and macrobursts during the JAWS Project reveal that the outflow intensity is independent of the reflectivity and visual appearance. Further analysis must be performed to find the mechanism that produces strong outflows in the wet cases. Possibly, misocyclones as modeled by Fujita and Wakimoto (1983b) or strong cyclonic (anti-cyclonic) shearing is important in microburst production.

Wind shear encountered by an aircraft may seriously affect its flight performance. When penetrating a microburst from the front or rear side, higher shear can be expected than penetrating from any other direction. However, Fig. 11 shows that wind shear is occuring in all directions, single-Doppler radar detection of microbursts is feasible and practical if installed near airport sites.

Acknowledgements:

The authors wish to thank Dr. T. Theodore Fujita for his guidance and for allowing us to use his photographs. Further thanks are given to Dr. Roger Wakimoto for his suggestions and to Mr. James Partacz for his assistance with the photographic work. This research has been sponsored by NSF under grant NSF/ATM 8109828, by NOAA under NA80AA-D-00001, and by NASA under grant NGR 14-001-008

REFERENCES

Fujita, T.T., and H.R. Byers, 1977: Spearhead echo and downburst in the crash of an airliner. Mon. Wea. Rev., 105, pp. 129-146

Fujita, T.T., and F. Caracena, 1977: An analysis of three weather-related aircraft accidents. Bull. Amer. Met. Soc., 58, pp. 1164-1181

Fujita, T.T., and R.M. Wakimoto, 1981: Five scales of airflow associated with a series of downbursts on 16 July 1980. Mon. Wea. Rev., 109, pp. 1438-1456

Fujita, T.T., and R.M. Wakimoto, 1983a: Microbursts in JAWS depicted by Doppler radars, PAM, and aerial photographs. Preprints, 21st Conf. on Radar Met., Edmonton, Amer. Met. Soc

Fujita, T.T., and R.M. Wakimoto, 1983b: JAWS microbursts revealed by triple-Doppler radar, aircraft, and PAM data. Preprints, 13th Conf. on Severe Local Storms, Tulsa, Amer. Met. Soc.

National Transportation Safety Board, 1983: Aircraft Accident Report: Pan American World Airways, Inc., Clipper 759, Boeing 727-235, N4737, New Orleans International Airport, Kenner, Louisiana, July 9, 1982. NTIS PB83-910402, 113pp.